

In Vitro Characterization of the Interaction between HIV-1 Gag and Human Lysyl-tRNA Synthetase*

Received for publication, February 7, 2006, and in revised form, May 1, 2006. Published, JBC Papers in Press, May 15, 2006, DOI 10.1074/jbc.M601189200

Brandie J. Kovaleski^{†1}, Robert Kennedy^{†1}, Minh K. Hong^{†1}, Siddhartha A. Datta[§], Lawrence Kleiman[¶], Alan Rein[§], and Karin Musier-Forsyth^{‡2}

From the [†]Department of Chemistry, University of Minnesota, Minneapolis, Minnesota 55455, the [§]Retrovirus Assembly Section, HIV Drug Resistance Program, NCI, National Institutes of Health, Frederick, Maryland 21702, and the [¶]Lady Davis Institute for Medical Research and McGill AIDS Centre, Jewish General Hospital, Montreal, Quebec H3T 1E2, Canada

Human immunodeficiency virus type 1 (HIV-1) viral assembly is mediated by multiple protein-protein and protein-nucleic acid interactions. Human tRNA^{Lys3} is used as the primer for HIV reverse transcription, and HIV Gag and GagPol are required for packaging of the tRNA into virions. Human lysyl-tRNA synthetase (LysRS) is also specifically packaged into HIV, suggesting a role for LysRS in tRNA packaging. Gag alone is sufficient for packaging of LysRS, and these two proteins have been shown to interact *in vitro* using glutathione *S*-transferase pull-down assays. *In vitro* pull-down assays using truncated constructs have also revealed that residues important for homodimerization of Gag and LysRS are critical for the Gag/LysRS interaction. In this work, we report further *in vitro* characterization of the interaction between HIV Gag and human LysRS using affinity pull-down assays, fluorescence anisotropy measurements and gel chromatography. An equilibrium binding constant of 310 ± 80 nM was measured for the Gag/LysRS interaction. We also show that capsid alone binds to LysRS with a similar affinity as full-length Gag. Point mutations that disrupt the homodimerization of LysRS and Gag *in vitro* do not affect their interaction. These results suggest that dimerization of each protein *per se* is not required for the interaction but that residues involved in forming the homodimer interfaces contribute to heterodimer formation. Gel chromatography studies further support the formation of a Gag/LysRS heterodimer.

HIV-1³ is a retrovirus, carrying its genetic information on single-stranded RNA (1). Once in the cytoplasm of the host cell,

the single-stranded viral RNA is reverse-transcribed into double-stranded DNA. Host-encoded tRNA^{Lys3} is the primer used by HIV-1 for initiation of reverse transcription (2). Newly synthesized proviral DNA translocates into the nucleus and is integrated into the host chromosomal DNA. Transcription of viral DNA yields spliced and unspliced mRNAs, progeny RNA genomes, and viral proteins. Among these viral proteins are two large precursor proteins, Gag and GagPol, both of which are translated from the same full-length viral RNA (3). During viral maturation, Gag is processed into the mature viral proteins: matrix, capsid (CA), and nucleocapsid. GagPol processing yields the mature HIV-1 enzymes: protease, reverse transcriptase, and integrase. In the last step of the viral life cycle, Gag, GagPol, genomic RNA, and specific host cell components assemble at plasma membranes and are eventually released from the cell.

Human tRNA^{Lys3}, one of the three major tRNA^{Lys} isoacceptors, is used as the primer for reverse transcription in HIV-1, although all three isoacceptors are selectively packaged into the newly forming virion (2, 4). Previous work has shown that packaging of tRNA^{Lys} requires GagPol (5), as well as human lysyl-tRNA synthetase (LysRS), which is also selectively packaged into HIV-1 (6). LysRS can be packaged into viral-like particles composed only of Gag, suggesting that interactions with Gag are both necessary and sufficient for LysRS incorporation (6).

Human LysRS is a class II synthetase, belonging to a closely related subgroup (IIb) with aspartyl- and asparaginyl-tRNA synthetases (7, 8). The crystal structures of *Escherichia coli* LysRS (9) and *Thermus thermophilus* LysRS (10) have been solved. LysRS is a homodimer, with each monomer consisting of an N-terminal anticodon binding domain, a dimerization domain formed by motif 1, and motifs 2 and 3 that together constitute the aminoacylation active site. LysRS is one of the most highly conserved synthetases, and sequence alignments suggest that prokaryotic and eukaryotic LysRSs are structurally very related (11).

Using wild-type (WT) and truncated HIV-1 Gag and LysRS variants, the regions critical for the protein-protein interaction have been mapped using *in vitro* glutathione *S*-transferase pull-down assays and *in vivo* LysRS packaging studies (12). The Gag/LysRS interaction depends on Gag sequences within the C-terminal domain (CTD) of CA and amino acids 208–259 in motif 1 of LysRS. Interestingly, these two regions contain elements involved in the formation of the dimerization interface of each

* This work was supported by National Institutes of Health Grant AI054145, National Institutes of Health Postdoctoral Grant GM069339 (to R. K.), and National Institutes of Health Predoctoral Training Grants T32-GM08277 (to M. K. H.) and T32-GM08700 (to B. J. K.). This work was also supported by the Intramural Research Program of the National Institutes of Health, National Cancer Institute, Center for Cancer Research. The costs of publication of this article were defrayed in part by the payment of page charges. This article must therefore be hereby marked "advertisement" in accordance with 18 U.S.C. Section 1734 solely to indicate this fact.

¹ These authors contributed equally to this work.

² To whom correspondence should be addressed: Dept. of Chemistry, University of Minnesota, 207 Pleasant St. SE, Minneapolis, MN 55455. Tel.: 612-624-0286; Fax: 612-626-7541; E-mail: musier@chem.umn.edu.

³ The abbreviations used are: HIV-1, human immunodeficiency virus type 1; WT, wild-type; LysRS, lysyl-tRNA synthetase; TrpRS, tryptophanyl-tRNA synthetase; Mut-LysRS, LysRS containing point mutations R247A, E265A, and F283A; WM-Gag, Δ p6-Gag containing point mutations W317A and M318A; CTD, C-terminal domain; CA, capsid protein; FPLC, fast performance liquid chromatography; HPLC, high performance liquid chromatography; AF, Alexa Fluor[®] 488 C₅ maleimide; FITC, fluorescein isothiocyanate;

NTA, nickel-nitrilotriacetic acid; β -ME, β -mercaptoethanol; MOPS, 4-morpholinepropanesulfonic acid; KMOPS, MOPS buffer with KOH.

HIV-1 Gag and Lysyl-tRNA Synthetase Interaction

protein. This suggests either that dimerization is critical for the interaction or that monomer units of each protein interact to form a heterodimeric Gag/LysRS complex.

In this report, we attempt to distinguish between these alternative models by constructing point mutants to disrupt homodimerization of LysRS and Gag. We characterize the interaction of WT and mutant proteins using *in vitro* affinity pull-down assays, fluorescence anisotropy, and gel chromatography. We also characterize the binding between LysRS and CA. Taken together, the results of this study lead to a refined model for the HIV-1 tRNA^{Lys}-packaging complex.

EXPERIMENTAL PROCEDURES

Plasmid Construction—Plasmid pM368 was constructed by cloning a 1.8-kbp fragment from pM116 into pKS583, a derivative of pET19b (11). The resultant plasmid produces a fusion protein that contains the N-terminal MRGSHHHHHSSGWVD sequence appended to full-length (1–597 amino acids) human LysRS and contains the genes conferring ampicillin and chloramphenicol resistance. The triple mutant (E265A,R247A,F283A) LysRS (Mut-LysRS) was constructed using the QuikChangeTM mutagenesis kit from Stratagene (La Jolla, CA) and the following primers: R247A, 5'-GTGATGATCTTAGACGCGATGATAA-ATTTCTGCCTCAC-3'; E265A, 5'-CATGGGAGTTTCAATC-GCTAGGAATCCCAGCTC-3'; and F283A, 5'-GTTGTGATA-AGTGATCGCAGGCTTGGCCACGGC-3'. The LysRS mutants were transformed into BL21(DE3) RIL-competent cells and screened by sequencing the entire gene, which also confirmed that no additional mutations were introduced during PCR.

Protein Purification—The following proteins were purified according to previously published procedures: T7 RNA polymerase (13), human prolyl-tRNA synthetase (ProRS) (14), and human LysRS (11). HIV-1 Δp6-Gag (Gag) and W317A/M318A mutant HIV-1 Δp6-Gag (WM-Gag) were prepared according to a previously published protocol (15, 16), except that buffer A consisted of 20 mM Tris·HCl, pH 7.4, 750 mM NaCl, 1 mM phenylmethylsulfonyl fluoride, 20 mM β-mercaptoethanol (β-ME), 1 mM tris(2-carboxyethyl)phosphine hydrochloride, 400 μM ZnCl₂, and 10% v/v glycerol. Mut-LysRS was prepared following the protocol for WT human LysRS (11).

The plasmid encoding histidine-tagged human TrpRS on a pET20b vector was a gift from Dr. Paul Schimmel (Scripps Research Institute, La Jolla, CA). BL21(DE3) cells transformed with the TrpRS expression vector were grown in LB containing 100 μg/ml ampicillin at 37 °C. Protein expression was induced at an A_{600 nm} of 0.4–0.6 by the addition of isopropyl-1-thio-β-D-galactopyranoside to a final concentration of 1 mM for 4 h at 37 °C. Cells were harvested by centrifugation, and the purification was performed on Ni²⁺-nitrilotriacetic acid (NTA) resin (Qiagen) equilibrated with 20 mM Tris·HCl, pH 8. TrpRS was eluted from the column using an imidazole gradient (30–250 mM) with TrpRS eluting at 100 mM imidazole. Purified TrpRS was then dialyzed against phosphate-buffered saline, concentrated, and diluted to 50% glycerol for storage at –80 °C. The final storage conditions were 10 mM NaPO₄, pH 7.4, 1.5 mM KPO₄, 3 mM KCl, 137 mM NaCl, and 50% glycerol.

The plasmid encoding HIV-1 CA (WISP98-85) was a gift from Dr. Wesley Sundquist (University of Utah, Salt Lake City,

UT). The expression and purification of CA was adapted from Sundquist and co-workers (17). BL21(DE3) cells transformed with the CA expression vector were grown in medium containing 100 μg/ml ampicillin at 37 °C. CA protein expression was induced at an A_{600 nm} of 0.8 by the addition of isopropyl-1-thio-β-D-galactopyranoside to a final concentration of 1 mM for 4 h. The cells were harvested by centrifugation, and the remaining steps were performed at 4 °C. Cells were resuspended in buffer B containing 20 mM KMOPS, pH 6.9, 5 mM β-ME, and two Complete mini protease inhibitor tablets (Roche Applied Science). Following sonication, cells were centrifuged at 10,000 × g for 30 min. CA was precipitated with 20% ammonium sulfate and exchanged into buffer B by dialysis using a 10,000 molecular weight cut off Slide-A-Lyzer cassette (Pierce). Purification was achieved by cation-exchange chromatography using SP-Sephacrose resin (Amersham Biosciences). CA was eluted using a 250-ml linear salt gradient (0–1 M NaCl) in buffer B. The purified protein, which typically eluted at 300 mM NaCl, was exchanged into 20 mM Tris·HCl, pH 8.0, and 5 mM β-ME. The concentrations of all proteins were determined by the Bradford method using the Bio-Rad protein assay kit and bovine serum albumin as the standard (18).

Fluorophore Labeling of Proteins—A solution of Alexa Fluor[®] 488 C₅ maleimide (AF) from Molecular Probes was prepared in dimethyl sulfoxide, and the concentration was determined using the extinction coefficient supplied by the manufacturer (ε_{493 nm} = 77,100 M⁻¹ cm⁻¹). Prior to labeling, LysRS, Mut-LysRS, or TrpRS were first incubated at room temperature for 15 min followed by elution through a 1-ml G50 Sephadex spin column to remove dithiothreitol. The proteins (40 μM) were labeled with AF at a 10:1 AF:protein ratio for 5 min on ice in 40 mM HEPES, pH 7.5, and 40 mM KCl. The reaction was quenched, and unreacted dye was removed by passing the labeling reaction through two 1-ml G50 Sephadex spin columns.

HIV-1 CA was labeled similarly, using fluorescein isothiocyanate (FITC). The concentration of the stock solution of FITC in dimethyl formamide was determined at pH >9 using the extinction coefficient ε_{494 nm} = 73,000 M⁻¹ cm⁻¹. The final labeling reaction was incubated for 15 min at room temperature. The final labeling stoichiometries for LysRS:AF, TrpRS:AF, Mut-LysRS:AF, and CA:FITC were estimated to be 2:1, 2:1, 1.5:1, and 1:1.6 fluorophore:protein, respectively. These values were determined by measuring the absorbance at 494 nm and using the extinction coefficients of the free fluorophores. Protein concentrations were estimated using the Bradford method (18). Samples were also subjected to 10% SDS-polyacrylamide gel electrophoresis. Ultraviolet illumination of the gels confirmed that our final labeled products had little or no free fluorophore.

tRNA^{Lys3} Preparation and Aminoacylation Activity—Unmodified WT tRNA^{Lys3} was prepared by *in vitro* transcription from FokI-digested plasmid pLYSF119 using T7 RNA polymerase as described previously (11). The extinction coefficient of 604,000 M⁻¹ cm⁻¹ was used to determine the concentration of all the tRNAs. Aminoacylation assays to test the activity of unlabeled and labeled LysRS and Mut-LysRS proteins were conducted as described previously (11). For WT LysRS and LysRS:AF488, assays contained 25 nM LysRS and tRNA^{Lys3} concentrations of 0.5 and 1.0 μM, respectively. For Mut-LysRS,

protein concentrations ranged from 0.025 to 1 μM , and tRNA^{Lys3} concentrations ranging from 0.5 to 2 μM were used.

Electrophoretic Band-shift Assay—The interaction between WT LysRS or Mut-LysRS and human tRNA^{Lys3} was measured using an electrophoretic band-shift assay. Dephosphorylation and 5'-³²P-end labeling of the tRNA^{Lys3} was performed using a modification of the method described earlier (19). Prior to 5'-end labeling, 20 μg of unmodified tRNA^{Lys3} was denatured for 2 min at 90 °C, cooled on ice, and incubated for 1 h at 60 °C with four units of bacterial alkaline phosphatase in 25 mM Tris-HCl, pH 8, 0.1% SDS, and 25% formamide. The dephosphorylated tRNA was then phenol/chloroform-extracted, ethanol-precipitated, and 5'-³²P-end-labeled by incubation with 30 units of phage T4 polynucleotide kinase (New England Biolabs) and 100 μCi of [γ -³²P]ATP for 30 min at 37 °C in the buffer supplied by the manufacturer. Labeled tRNA was purified by electrophoresis on a 12% denaturing polyacrylamide gel.

Labeled tRNA^{Lys3} (4.5 μM) was incubated with different concentrations of either WT LysRS or Mut-LysRS (0.15, 0.375, 0.75, or 1.5 μM) in 20 mM Tris-HCl, pH 7.4, 50 mM NaCl, 0.1 mM EDTA, and 5% glycerol for 20 min at room temperature and analyzed by electrophoresis at 4 °C on a 5% Tris-borate-EDTA non-denaturing polyacrylamide gel prepared with 0.25 \times Tris-borate-EDTA (22.5 mM Tris-borate and 0.25 mM EDTA) and 0.5 \times Tris-borate-EDTA running buffer. The gels were visualized using a Bio-Rad molecular imager FX, and band densities of free and bound tRNA^{Lys3} were determined using Quantity One software. Equilibrium binding constants were determined by fitting these data to a standard hyperbolic curve using Kaleidagraph.

Gel Chromatography—The oligomeric states of WT LysRS and Mut-LysRS in the absence of Gag were initially monitored by size-exclusion chromatography using a Superose 12 column (Amersham Biosciences) attached to an Amersham Biosciences fast performance liquid chromatography (FPLC) system. The mobile phase was 50 mM NaPO₄, pH 7, 150 mM NaCl, and 10 mM β -ME. The column was calibrated using molecular mass markers ranging from 13.7 to 440 kDa (Amersham Biosciences). A 2.5 μM solution of WT LysRS or Mut-LysRS was loaded onto the column, and protein absorbance at 280 nm was monitored.

The monomer-dimer equilibrium of WT LysRS and Mut-LysRS was analyzed by elution through a Bio-Sil 250-5 size-exclusion column (Bio-Rad) attached to a Beckman high performance liquid chromatography (HPLC) system. The mobile phase was 50 mM NaPO₄, pH 7.5, and 150 mM NaCl. The column was calibrated using gel chromatography molecular weight mass ranging from 1.35 to 670 kDa (Bio-Rad). To esti-

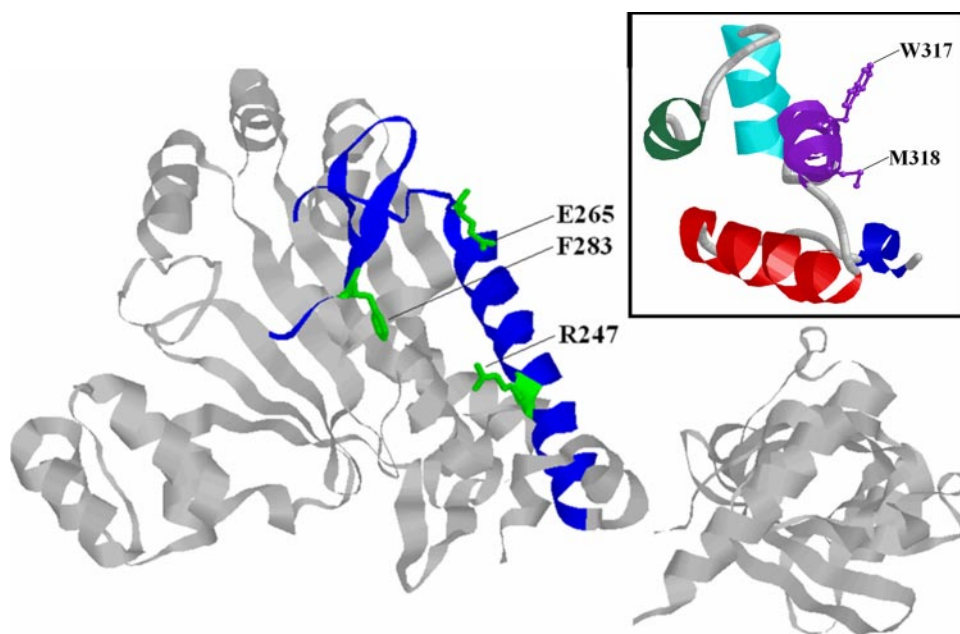


FIGURE 1. Structure of the *E. coli* LysRS monomer (9) (PDB reference: 1LYL). Motif 1, the dimerization domain, is colored blue. The three residues that were mutated to alanine to generate Mut-LysRS are in green (Arg-247, Glu-265, Phe-283). *Inset*, ribbon diagram of the CA CTD monomer (33) (PDB reference: 1BAJ). Secondary structures are color-coded as follows: blue, 3₁₀ helix; red, α -helix 1; purple, α -helix 2; cyan, α -helix 3; green, α -helix 4. The two residues that were mutated to alanine to generate WM-Gag are labeled.

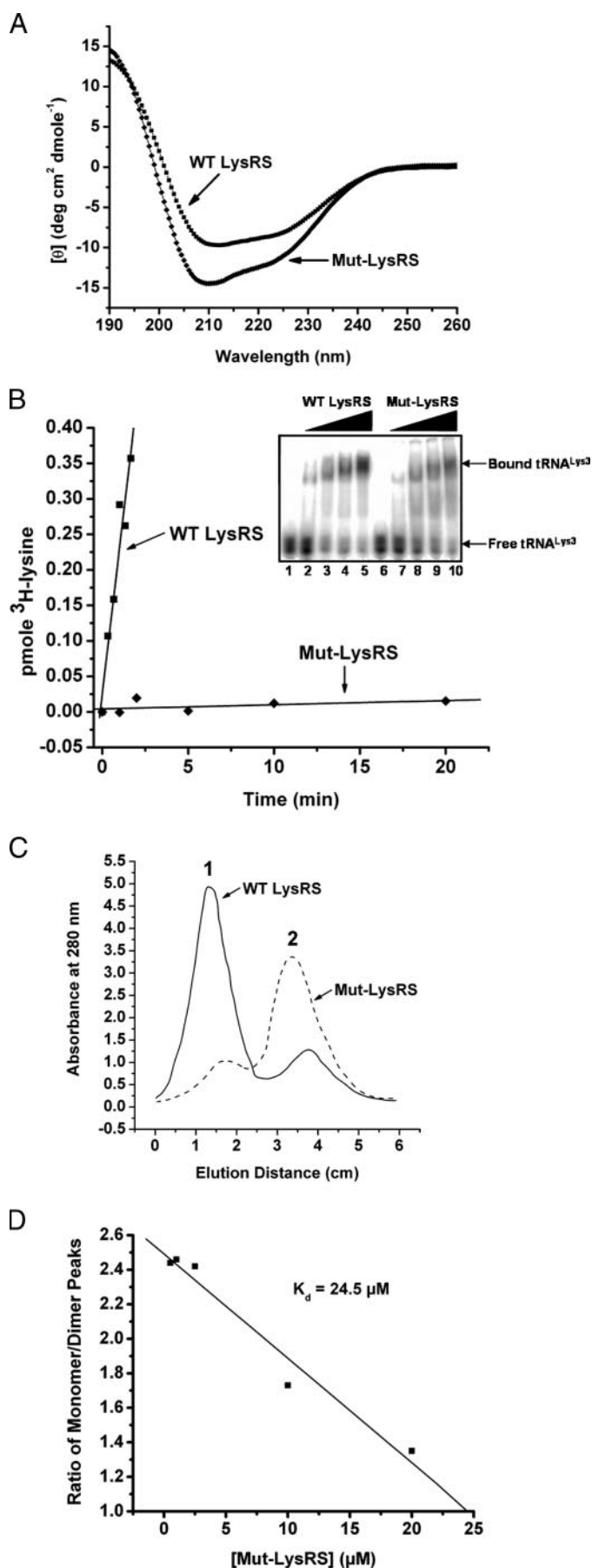
mate monomer-dimer equilibrium dissociation constants, solutions of each protein ranging from 0.5 to 20 μM were loaded onto the column, and protein absorbance at 280 nm was monitored. The areas under the monomer and dimer peaks were quantified using Beckman PACE 32 Karat software version 4.0, and the peak ratios were plotted versus Mut-LysRS concentration. The K_d was assumed to be the concentration at which we observed a 1:1 ratio of monomer to dimer peaks.

The interaction between LysRS and Gag was analyzed by size-exclusion FPLC carried out at 4 °C using a Superose 12 column (Amersham Biosciences). The mobile phase was 50 mM NaPO₄, pH 7, and 150 mM NaCl. Solutions of LysRS alone (15 μM), Gag alone (40 μM), and LysRS/Gag (15 μM /40 μM) were incubated in mobile phase buffer at room temperature for 2 h. Each sample (100 μl) was injected separately on the column, and protein elution was monitored at 280 nm. The traces were digitized using Origin 7 software (Microcal). Fractions (250 μl) were collected every 30 s and analyzed by 10% SDS-polyacrylamide gel electrophoresis. Gels were stained with Coomassie Brilliant Blue and scanned to visualize the bands.

Circular Dichroism Analysis—CD spectra were measured at room temperature using a J-710 spectropolarimeter (Jasco) with a 0.1-cm path-length cuvette. Prior to analysis, proteins were dialyzed into 10 mM NaPO₄, pH 7.5, and diluted to a concentration of 5 μM . Spectra were accumulated over six scans.

In Vitro Pull-down Assays—Purified human LysRS, Mut-LysRS, human TrpRS, human ProRS, HIV-1 Gag, WM-Gag, and CA were dialyzed against binding/dialysis buffer containing 25 mM NaPO₄, pH 7, 125 mM NaCl, 2.5 mM β -ME at 4 °C. The histidine-tagged LysRS or TrpRS (250 μg) were incubated with 25 μl of Ni²⁺-NTA resin in a volume of 125 μl for 1 h at room temperature. The resin was washed once

HIV-1 Gag and Lysyl-tRNA Synthetase Interaction



with binding/dialysis buffer to remove any unbound LysRS, TrpRS, or ProRS. The dialyzed Gag, WM-Gag, or CA (125 μg in a volume of 150 μl) was added to the LysRS or TrpRS bound to Ni^{2+} -NTA and incubated for 2 h at room temperature. As a control, a similar binding experiment was performed in the absence of bound synthetase. The resin was then washed once with binding/dialysis buffer to remove any unbound protein followed by six washes with binding/dialysis buffer containing 10 mM imidazole to remove any protein non-specifically bound to the resin. To elute the bound protein, the resin was incubated in 150 μl of binding/dialysis buffer containing 200 mM imidazole for 1 h at room temperature, eluted from the resin by centrifugation, and diluted with 2 \times gel loading buffer containing 50 mM Tris-HCl, pH 6.8, 100 mM β -ME, 2% SDS, 0.1% bromphenol blue, and 10% glycerol.

Samples were run on a 10 or 12% SDS-polyacrylamide gel followed by transfer onto a polyvinylidene fluoride Immobilon-P membrane (Millipore). Gag, WM-Gag, and CA were detected using a polyclonal antibody for HIV-1 CA from Pocono Rabbit Farm and Laboratory. A goat anti-rabbit horseradish peroxidase conjugate (Bio-Rad) was used as the secondary antibody. Detection was performed by enhanced chemiluminescence using Western blotting detection reagents from Amersham Biosciences.

Fluorescence Anisotropy Measurements—Equilibrium dissociation constants were determined by measuring the fluorescence anisotropy of 50 nM fluorescently labeled protein (LysRS:AF, TrpRS:AF, Mut-LysRS:AF, or CA:FITC) as a function of increasing concentrations of an unlabeled protein (LysRS, TrpRS, Mut-LysRS, Gag, or WM-Gag). The labeled protein was incubated with varying amounts of the desired unlabeled protein for 30 min at room temperature in 40 mM HEPES, pH 7.5, and 50 mM NaCl. Anisotropy measurements were made on a Photon Technology International spectrofluorimeter (Model QM-2000). The excitation and emission wavelengths were 490 and 520 nm, respectively (slit widths = 5 nm).

Anisotropy was measured using the time-based function for 30 s (integration time = 1 s; resolution = 8 s), and the data were averaged. All measurements were carried out at least three times. The titration curves were fit to the following equation, which assumes a 1:1 binding stoichiometry (20–22),

$$A = A_{\min} + \frac{[(Y + S + K_d) - \{(Y + S + K_d)^2 - (4YS)\}^{1/2}]}{2Y} \cdot (A_{\max} - A_{\min}) \quad (\text{Eq. 1})$$

where A is the measured anisotropy at a particular total concentration of the unlabeled protein (S) and the labeled protein

FIGURE 2. Characterization of Mut-LysRS. *A*, CD spectra of WT LysRS (■) versus Mut-LysRS (◆). *B*, aminoacylation assay comparing activity of WT LysRS (25 nM, ■) and Mut-LysRS (1 μM , ◆). tRNA^{Lys} concentrations were 0.5 μM for WT LysRS and 2 μM for Mut-LysRS. *Inset*, electrophoretic band-shift assay showing the interaction between $\text{tRNA}^{\text{Lys3}}$ and WT or Mut-LysRS. ^{32}P -labeled $\text{tRNA}^{\text{Lys3}}$ was incubated with different concentrations of either WT or Mut-LysRS: 0 μM (lanes 1 and 6), 0.15 μM (lanes 2 and 7), 0.375 μM (lanes 3 and 8), 0.75 μM (lanes 4 and 9), or 1.5 μM (lanes 5 and 10). *C*, gel chromatography of WT LysRS (solid line) and Mut-LysRS (dotted line). *Peak 1* corresponds to dimeric LysRS, and *peak 2* corresponds to monomeric LysRS. *D*, determination of monomer-dimer equilibrium dissociation constant for Mut-LysRS by gel chromatography.

(Y), A_{\min} is the minimum anisotropy, A_{\max} is the final maximum anisotropy, and K_d is the dissociation constant.

RESULTS

Design and Characterization of Monomeric LysRS and Gag—

To investigate whether monomeric forms of human LysRS and Gag could interact, we designed variants containing point mutations in the known dimerization motif of each protein using the three-dimensional structure of *E. coli* LysRS as a model for the human synthetase (9). Fig. 1 shows the residues in the motif 1 dimerization domain, Arg-247, Glu-265, Phe-283, that were mutated to alanine to generate Mut-LysRS. These residues are highly conserved in known LysRS sequences and participate in interactions that appear to stabilize the dimer interface. The triple mutant was successfully overexpressed and purified. CD analysis indicated that the secondary structure of Mut-LysRS was similar to that of WT LysRS (Fig. 2A). Class II synthetases require homodimerization for aminoacylation function (23). Thus, if the mutations do in fact disrupt dimerization, Mut-LysRS should show little or no aminoacylation activity. Fig. 2B shows that even at high concentrations of Mut-LysRS, the triple mutant lacks aminoacylation activity, consistent with this expectation. Using an electrophoretic band-shift assay, Mut-LysRS was also tested for its ability to bind tRNA^{Lys}. Although it lacked aminoacylation activity, the triple mutant still bound tRNA with a similar affinity (~670 nM) as WT LysRS (~430 nM) (Fig. 2B, inset).

Gel chromatography experiments performed with WT LysRS and Mut-LysRS were also consistent with a shift in the equilibrium distribution toward monomeric species for the triple mutant (Fig. 2C). By carrying out gel chromatography as a function of Mut-LysRS concentration, we estimated the dissociation constant for the monomer-dimer equilibrium to be 24.5 μM (Fig. 2D). Similar experiments performed with WT LysRS showed that it remained primarily dimeric at all concentrations tested (data not shown). Based on these data, the monomer-dimer equilibrium dissociation constant of WT LysRS is <200 nM. Taken together, these data support successful disruption of interactions that are critical for dimerization in the triple mutant.

Individual mutations of W184A and M185A in the CTD of CA have been reported to prevent CA dimerization *in vitro* (24). In addition, the same individual mutations in the context of Gag, W317A and M318A, inhibit Gag-Gag interactions (25). In this study, we simultaneously mutated both of these residues

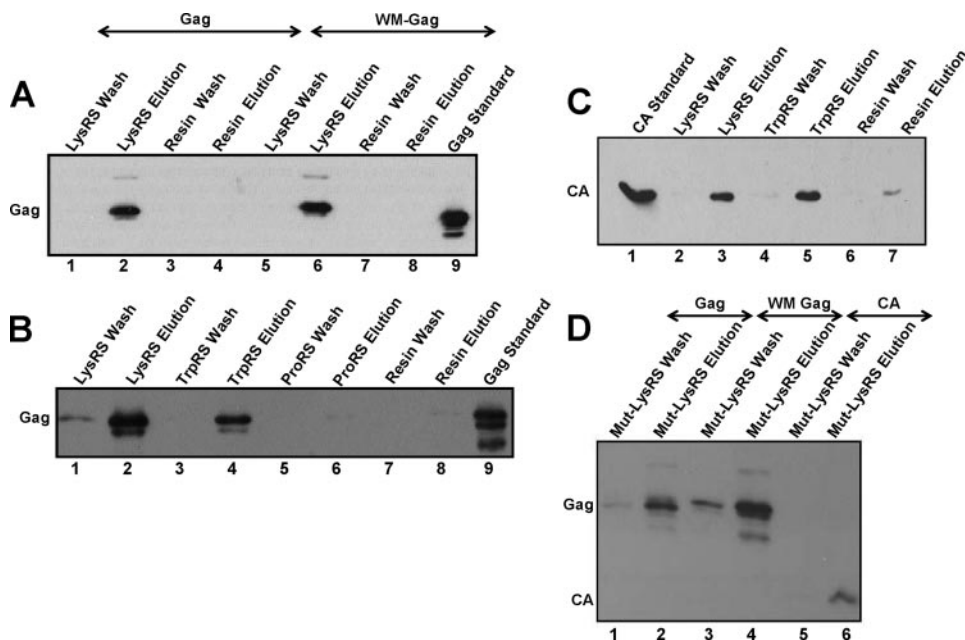


FIGURE 3. *In vitro* pull-down assays. Purified histidine-tagged LysRS, Mut-LysRS, TrpRS, or ProRS were absorbed to Ni^{2+} -NTA resin and incubated with purified Gag, WM-Gag, or CA. Samples were run on a 10 or 12% SDS-polyacrylamide gel, subjected to Western blot analysis, and probed with anti-CA antibody. *A*, interaction between WT LysRS and Gag (lanes 1 and 2) or WM-Gag (lanes 5 and 6). Lanes 2, 4, 6, and 8 correspond to the final elution in the presence (lanes 2 and 6) or absence (lanes 4 and 8) of LysRS. Lane 9 is a Gag standard. The Wash lanes correspond to the final wash fraction in each experiment. The Resin lanes correspond to a negative control in which Gag or WM-Gag was incubated with just the Ni^{2+} -NTA resin to test for nonspecific binding. *B*, interaction between Gag and WT LysRS (lanes 1 and 2), TrpRS (lanes 3 and 4), ProRS (lanes 5 and 6), and no synthetase as a negative control (lanes 7 and 8). Lane 9 is a Gag standard. *C*, interaction between CA and WT LysRS (lanes 2 and 3) or TrpRS (lanes 4 and 5). Lane 1 is a CA standard. The Resin lanes correspond to a negative control in which CA was incubated with just Ni^{2+} -NTA resin to test for nonspecific binding (lanes 6 and 7). *D*, interaction between Mut-LysRS and Gag (lanes 1 and 2), WM-Gag (lanes 3 and 4), or CA (lanes 5 and 6). The positions of protein standards are indicated on the left of the gel.

to alanine to generate WM-Gag. Fig. 1 (inset) shows the location of these residues in the CTD of CA. Using sedimentation equilibrium experiments, the monomer association constants were determined to be 5.5 μM for WT Δp6 -Gag and >20 μM for WM-Gag.⁴ These results support significant disruption of Gag-Gag interactions in the double mutant.

Characterization of the Fluorescently Labeled Proteins—To confirm that the fluorescently labeled synthetases were properly folded and active, we measured the aminoacylation activity of labeled and unlabeled proteins. No detectable difference in the efficiency of aminoacylation relative to unlabeled protein was observed for LysRS:AF or TrpRS:AF (data not shown). Although we were unable to test an enzymatic activity for CA:FITC, CD analysis showed no difference in the secondary structure of CA:FITC relative to unlabeled CA (data not shown).

In Vitro Affinity Pull-down Assays—Purified histidine-tagged LysRS, Mut-LysRS, TrpRS, or ProRS were absorbed to Ni^{2+} -NTA resin and incubated with Gag, WM-Gag, or CA. Following extensive washing to remove non-specifically bound protein, the material on the resin was eluted with 200 mM imidazole and subjected to SDS-polyacrylamide gel electrophoresis and immunoblot analysis.

LysRS pulls down both Gag and WM-Gag to similar extents (Fig. 3A, lanes 2 and 6). Negative control experiments per-

⁴ S. A. K. Datta, Z. Zhao, P. K. Clark, S. Tarasov, J. N. Alexandratos, S. J. Campbell, M. Kvaratskhelia, J. Lebowitz, and A. Rein, manuscript in preparation.

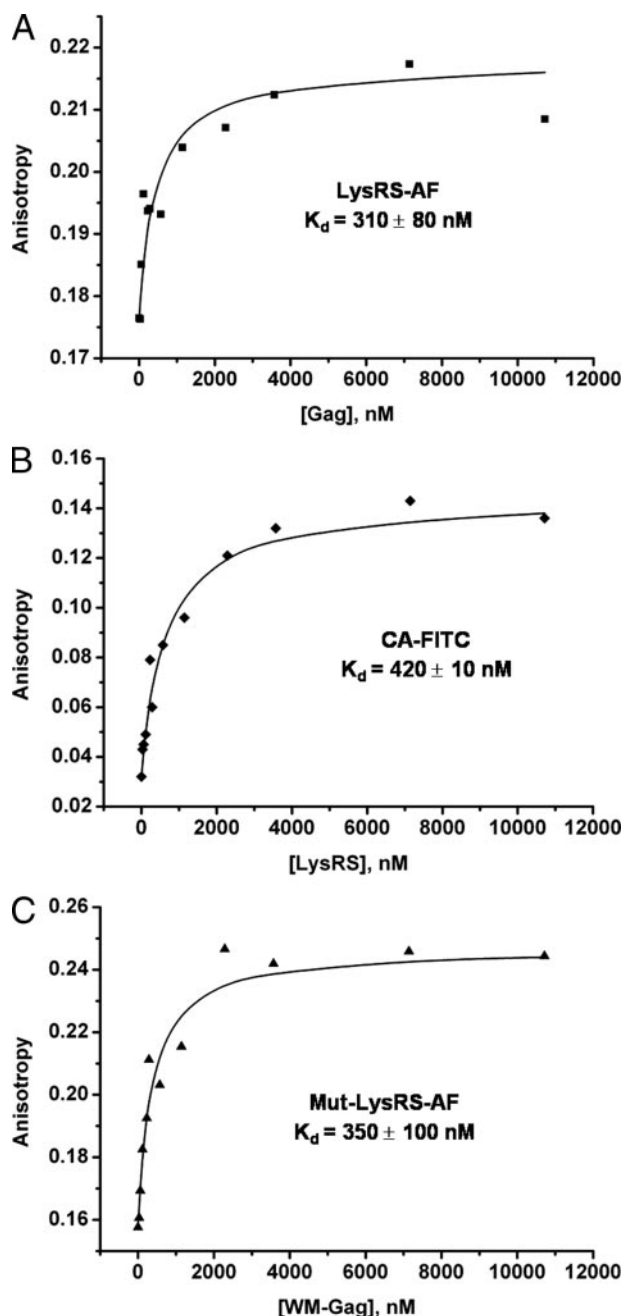


FIGURE 4. **Fluorescence anisotropy experiments.** The binding affinities of WT LysRS to Gag (A) or CA (B) and Mut-LysRS to WM-Gag (C) were measured using 50 nM fluorescently labeled protein as a function of increasing concentrations of the interacting (unlabeled) protein. The data were fit to Equation 1 given under "Experimental Procedures." Only a representative data set is shown, but all measurements were carried out at least three times with the standard deviation indicated (see also Table 1).

formed with Gag or WM-Gag in the absence of LysRS did not yield a Gag signal (Fig. 3A, lanes 4 and 8). This demonstrates that Gag and WM-Gag do not bind to the Ni^{2+} -NTA resin in the absence of LysRS. The final wash fractions were also examined by SDS-polyacrylamide gel electrophoresis and immunoblot analysis and contained no protein (Fig. 3A, lanes 1, 3, 5, and 7).

A pull-down experiment designed to test the specificity of the LysRS/Gag interaction was carried out using human TrpRS

TABLE 1

Equilibrium dissociation constants (K_d) obtained from fluorescence anisotropy measurements

Measurements were performed in the presence of 40 mM HEPES, pH 7.5, and 50 mM NaCl. Results are the average of three trials with the standard deviation shown.

Labeled protein	Interacting protein	K_d
		<i>nM</i>
LysRS-AF	Gag	310 ± 80
	WM-Gag	590 ± 70
Mut-LysRS-AF	Gag	770 ± 100
	WM-Gag	350 ± 100
TrpRS-AF	Gag	1550 ± 290
CA-FITC	LysRS	420 ± 10
	LysRS/tRNA ^{Lys3}	370 ± 60
	Mut-LysRS	530 ± 60
	TrpRS	1620 ± 280

and human ProRS (Fig. 3B). We observe that both LysRS and TrpRS were able to bind and pull down Gag, although the interaction with TrpRS appeared to be weaker (Fig. 3B, lanes 2 and 4). No signal was observed in the case of ProRS (Fig. 3B, lane 6).

The critical region for the LysRS interaction was previously mapped to amino acids 323–362 of Gag, located in the CTD of CA (12). To investigate whether the CA domain of Gag was sufficient for an interaction with LysRS, a pull-down experiment was performed using immobilized WT LysRS or TrpRS and CA (Fig. 3C). Both LysRS (lane 3) and TrpRS (lane 5) could pull down CA, showing that this domain of Gag is sufficient for the interaction. Negative control experiments performed with CA in the absence of synthetase did not show significant binding (Fig. 3C, lanes 6 and 7).

Mut-LysRS was also tested for its ability to pull down Gag, WM-Gag, and CA. Based on the concentration of Mut-LysRS applied to the column (25 μM), at least 50% is expected to be monomeric. The results shown in Fig. 3D (lanes 2, 4, and 6) show that Mut-LysRS is able to interact with all three proteins tested.

Characterization of Binding Affinity—Fluorescence anisotropy experiments were used to determine equilibrium dissociation constants (K_d) for LysRS and Mut-LysRS binding to Gag, WM-Gag, and CA. The binding curve obtained for the WT LysRS:AF/Gag complex is shown in Fig. 4A. The data were fit to a binding model that assumes 1:1 binding stoichiometry, and an apparent K_d of 310 ± 80 nM was determined. An ~ 5 -fold higher K_d of 1550 ± 290 nM was measured for the TrpRS:AF/Gag complex (Table 1). We were unable to detect an interaction between ProRS:AF and Gag using this assay.

Both LysRS and TrpRS also bound to CA, but once again, a 4-fold higher K_d was measured for the TrpRS/CA complex relative to the LysRS/CA complex (Table 1). The affinity of the CA:FITC/LysRS interaction (420 ± 10 nM, Fig. 4B) is similar to that of the LysRS:AF/Gag interaction, in accord with the finding that the Gag/LysRS interaction is dependent on residues in the CA domain of Gag (12). Interestingly, binding of CA to LysRS was independent of the concentration of monovalent cations over the range 50–500 mM NaCl (data not shown). This suggests that the protein-protein interaction between LysRS and CA is not ionic in nature.

Packaging of LysRS into HIV-1 or virus-like particles occurs independently of tRNA^{Lys} packaging (6). To test whether tRNA affects the LysRS/CA interaction, we added an equal molar

ratio of tRNA^{Lys3} to the LysRS used in the titration experiment with CA:FITC. The calculated binding affinity (370 ± 60 nM, Table 1) revealed that the CA:FITC/LysRS interaction was not substantially altered by the addition of tRNA.

The binding affinity determined for the Mut-LysRS:AF/WM-Gag complex (350 ± 100 nM, Fig. 4C) was similar to the affinity measured for the WT proteins. Based on the known strength of the homodimer interactions, these experiments were conducted under conditions in which both proteins are expected to be monomeric (50 nM Mut-LysRS and ≤ 12 μ M WM-Gag). In addition, the affinities of monomeric LysRS or Gag for the corresponding WT proteins (Mut-LysRS/Gag, Mut-LysRS/CA, and LysRS/WM-Gag) were ~ 2 -fold greater (770 ± 100 nM, 530 ± 60 nM, and 590 ± 70 nM, respectively, Table 1) than the affinities between the two monomeric proteins or the two WT proteins.

Gel Chromatography Analysis of Heterodimer Formation—The stoichiometry of the LysRS/Gag interaction was further investigated by gel chromatography. Fig. 5A shows the results of three separate experiments performed following a 2-h incubation of the proteins either alone or together. LysRS alone ($MW_{\text{dimer}} = 138$ kDa) results in the appearance of a major peak eluting at 25 min, likely corresponding to a LysRS dimer (*peak 1*, apparent molecular mass = 160 kDa). Gag alone ($MW_{\text{dimer}} = 100$ kDa) results in the appearance of a single major peak eluting at 33 min, likely corresponding to a Gag dimer (*peak 3*, apparent molecular mass = 110 kDa). When both LysRS and Gag were incubated together at room temperature for 2 h, an additional species appeared at 31 min (*peak 2*, apparent molecular mass = 125 kDa). The predicted molecular mass of a LysRS/Gag heterodimer (119 kDa) is consistent with peak 2. Importantly, there is no appearance of a new species with molecular mass greater than the LysRS dimer, ruling out the formation of a LysRS/Gag $\alpha_2\beta_2$ complex.

To confirm that both proteins were present in peak 2, fractions from each of the three samples were collected every 30 s and analyzed by 10% SDS-polyacrylamide gel electrophoresis. Fig. 5B shows the fractions that eluted at 29.5–32 min. Although the LysRS-only (Fig. 5B, *top*) and the Gag-only (Fig. 5B, *bottom*) samples contain very little protein in the 31-min fraction, both proteins are clearly present in this fraction in the sample in which they were incubated together (Fig. 5B, *middle*). Thus, peak 2 is not the result of a shift in the elution of one of the individual proteins, and this result strongly supports the formation of a heterodimeric LysRS/Gag complex.

DISCUSSION

The proposed model for human tRNA^{Lys} packaging into HIV-1 involves an assembly complex formed between genomic RNA, Gag, Gag-Pol, tRNA^{Lys}, and human LysRS (26). The details of the molecular interactions between the components of this packaging complex are not known. As a first step toward this goal, we have begun to characterize the interaction between human LysRS and Gag, which occurs independent of the other components. The strength of the interaction between the WT proteins ($K_d = 310 \pm 80$ nM) is unaffected by the presence of tRNA. The interaction was previously local-

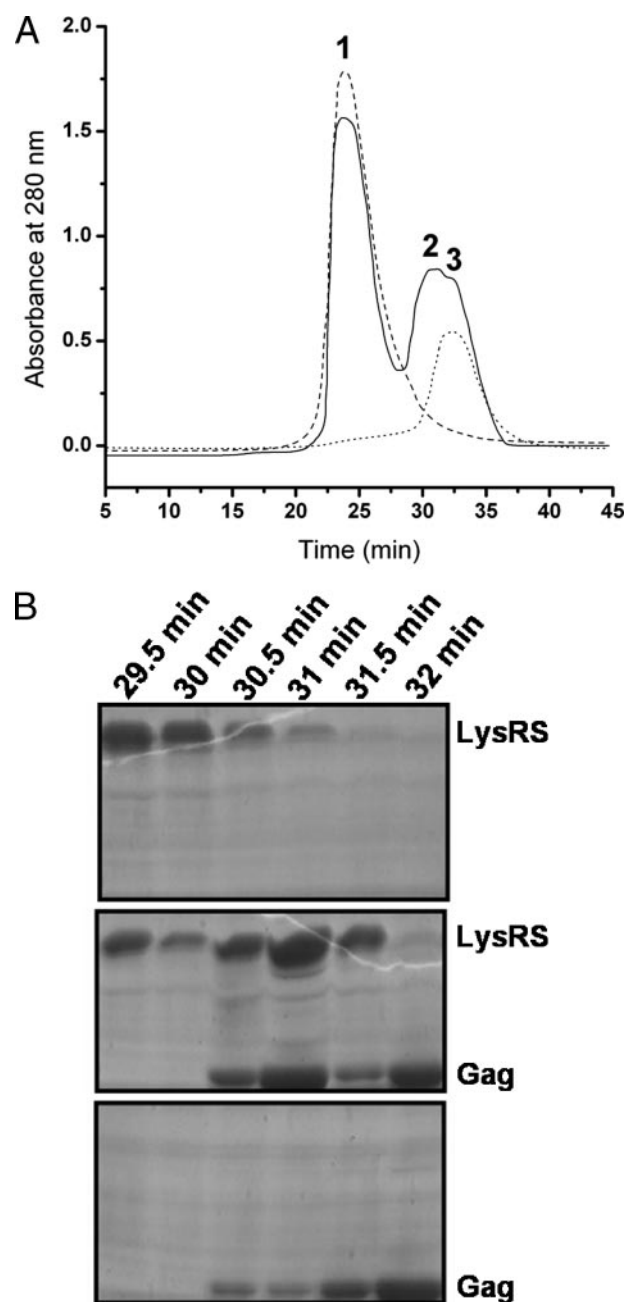


FIGURE 5. Gel chromatography FPLC analysis. LysRS and Gag were applied to a Superose 12 FPLC column either individually or following incubation together as described under "Experimental Procedures." *A*, chromatograms of LysRS alone (*dashed line*), Gag alone (*dotted line*), or LysRS/Gag (*solid line*) following a 2-h incubation. *B*, scan of a Coomassie Brilliant Blue stained 10% SDS-polyacrylamide gel showing the collected fractions from 29.5 to 32 min for samples containing LysRS alone (*top*), LysRS/Gag incubated together (*middle*), and Gag alone (*bottom*).

ized to the CTD of CA (12), and indeed, our data show that the CA protein interacts with LysRS with a similar affinity as Gag.

The Gag/LysRS interaction depends on the dimerization motif of each protein (12). We show here that dimerization of each of the interacting partners can be disrupted by site-directed mutagenesis without significantly affecting the strength of the protein-protein interaction. These results raise the possibility that there is a slow interconversion of monomers and dimers, with the heterodimer formed only from LysRS and/or

HIV-1 Gag and Lysyl-tRNA Synthetase Interaction

Gag in the monomeric state. Since our K_d calculations used the concentration of total Gag and LysRS present in solution, the calculated value represents an upper limit for the dissociation constant, which may be significantly lower for monomeric wild-type proteins. Nevertheless, taken together, these results suggest that homodimerization *per se* is not critical for the Gag/LysRS interaction but that a similar, although probably not identical, interface may be used for the hetero-protein interaction. Consistent with this idea, recent structural studies of a mammalian SCAN domain dimer, a homolog of the HIV-1 CA CTD, suggest that the interaction domain of CA is somewhat plastic and can adopt a different dimerization interface by swapping the major homology region element between monomers (27). This plasticity is likely advantageous as CA must participate in a wide variety of interactions throughout the viral life cycle (28).

Gel chromatography studies performed here in the absence of RNA are consistent with a Gag/LysRS complex size corresponding to a heterodimer. No evidence for a higher molecular weight complex was obtained (e.g. a dimer of dimers). The interaction between CA monomers has been reported to be relatively weak ($K_d = 18 \mu\text{M}$) (24). The interaction between Gag monomers is similarly weak.⁴ In contrast, the interaction between monomers in the LysRS homodimer is quite strong ($K_d < 200 \text{ nM}$). The precise mechanism of heterodimer formation is not clear and may involve other factors that serve to help disrupt the LysRS homodimer.

The specificity of the Gag/LysRS interaction was previously probed *in vivo* by examining the packaging of other synthetases into HIV-1 virions (29). Of the eight synthetases examined, only LysRS was found in HIV-1 (29). TrpRS was not detected in HIV-1. Conversely, in avian Rous sarcoma virus, which uses tRNA^{Trp} as a primer, TrpRS is found, whereas LysRS is not present (30–32). Whether this incorporation specificity in HIV-1 can be accounted for by the 5-fold reduction in the affinity of TrpRS for HIV-1 Gag when compared with LysRS is not certain, and other parameters, such as cellular factors or cellular compartmentalization, may contribute to the specificity of incorporation of LysRS into HIV-1. We were unable to detect an interaction between human ProRS and Gag in our *in vitro* studies. This synthetase is not found in HIV-1 (4) and is also not packaged into murine leukemia virus despite the fact that tRNA^{Pro} is the primer in the murine system (32). The molecular interaction between motif 1 of LysRS and the CTD of CA represents a new target for anti-retroviral therapy, and studies to more finely map the residues involved in the protein-protein interaction are currently underway.

Acknowledgments—We acknowledge and give special thanks to Dr. Whyte G. Owen (Mayo Clinic, Rochester, MN) for providing valuable insight and assistance with the HPLC analysis of the LysRS/Gag interaction. We thank Dr. Kristen M. Stewart and Dr. Sanchita Hati for purification of human TrpRS and human ProRS, respectively.

REFERENCES

1. Vogt, V. M. (1997) in *Retroviruses* (Coffin, J. M., Hughes, S. M., and Varmus, H. E., eds), pp. 27–69, Cold Spring Harbor Laboratory Press, Plainview, NY
2. Jiang, M., Mak, J., Ladha, A., Cohen, E., Klein, M., Rovinski, B., and Kleiman, L. (1993) *J. Virol.* **67**, 3246–3253
3. Swanstrom, R., and Wills, J. W. (1997) in *Retroviruses* (Coffin, J. M., Hughes, S. M., and Varmus, H. E., eds), pp. 263–334, Cold Spring Harbor Laboratory Press, Plainview, NY
4. Mak, J., and Kleiman, L. (1997) *J. Virol.* **71**, 8087–8095
5. Mak, J., Jiang, M., Wainberg, M. A., Hammarskjold, M. L., Rekosh, D., and Kleiman, L. (1994) *J. Virol.* **68**, 2065–2072
6. Cen, S., Khorchid, A., Javanbakht, H., Gabor, J., Stello, T., Shiba, K., Musier-Forsyth, K., and Kleiman, L. (2001) *J. Virol.* **75**, 5043–5048
7. Eriani, G., Delarue, M., Poch, O., Gangloff, J., and Moras, D. (1990) *Nature* **347**, 203–206
8. Eriani, G., Dirheimer, G., and Gangloff, J. (1990) *Nucleic Acids Res.* **18**, 7109–7118
9. Onesti, S., Miller, A. D., and Brick, P. (1995) *Structure (Lond.)* **3**, 163–176
10. Cusack, S., Yaremchuk, A., and Tukalo, M. (1996) *EMBO J.* **15**, 6321–6334
11. Shiba, K., Stello, T., Motegi, H., Noda, T., Musier-Forsyth, K., and Schimmel, P. (1997) *J. Biol. Chem.* **272**, 22809–22816
12. Javanbakht, H., Halwani, R., Cen, S., Saadatmand, J., Musier-Forsyth, K., Gottlinger, H., and Kleiman, L. (2003) *J. Biol. Chem.* **278**, 27644–27651
13. Ellinger, T., and Ehrlich, R. (1998) *BioTechniques* **24**, 718–720
14. Forsyth, C. J., Heacock, D., Shiba, K., and Musier-Forsyth, K. (1996) *Bioorg. Chem.* **24**, 273–289
15. Campbell, S., and Vogt, V. M. (1997) *J. Virol.* **71**, 4425–4435
16. Campbell, S., and Rein, A. (1999) *J. Virol.* **73**, 2270–2279
17. Yoo, S., Myszk, D. G., Yeh, C., McMurray, M., Hill, C. P., and Sundquist, W. I. (1997) *J. Mol. Biol.* **269**, 780–795
18. Bradford, M. M. (1976) *Anal. Biochem.* **72**, 248–254
19. Isel, C., Ehresmann, C., Keith, G., Ehresmann, B., and Marquet, R. (1995) *J. Mol. Biol.* **247**, 236–250
20. Reid, S. L., Parry, D., Liu, H. H., and Connolly, B. A. (2001) *Biochemistry* **40**, 2484–2494
21. Muller, B., Restle, T., Reinstein, J., and Goody, R. S. (1991) *Biochemistry* **30**, 3709–3715
22. Lundblad, J. R., Laurance, M., and Goodman, R. H. (1996) *Mol. Endocrinol.* **10**, 607–612
23. Cusack, S. (1995) *Nat. Struct. Biol.* **2**, 824–831
24. Gamble, T. R., Yoo, S., Vajdos, F. F., von Schwedler, U. K., Worthylyake, D. K., Wang, H., McCutcheon, J. P., Sundquist, W. I., and Hill, C. P. (1997) *Science* **278**, 849–853
25. Burniston, M. T., Cimarelli, A., Colgan, J., Curtis, S. P., and Luban, J. (1999) *J. Virol.* **73**, 8527–8540
26. Kleiman, L., Halwani, R., and Javanbakht, H. (2004) *Curr. HIV Res.* **2**, 163–175
27. Ivanov, D., Stone, J. R., Maki, J. L., Collins, T., and Wagner, G. (2005) *Mol. Cell* **17**, 137–143
28. von Schwedler, U. K., Stray, K. M., Garrus, J. E., and Sundquist, W. I. (2003) *J. Virol.* **77**, 5439–5450
29. Halwani, R., Cen, S., Javanbakht, H., Saadatmand, J., Kim, S., Shiba, K., and Kleiman, L. (2004) *J. Virol.* **78**, 7553–7564
30. Cen, S., Javanbakht, H., Kim, S., Shiba, K., Craven, R., Rein, A., Ewalt, K., Schimmel, P., Musier-Forsyth, K., and Kleiman, L. (2002) *J. Virol.* **76**, 13111–13115
31. Sawyer, R. C., and Dahlberg, J. E. (1973) *J. Virol.* **12**, 1226–1237
32. Waters, L. C., and Mullin, B. C. (1977) *Prog. Nucleic Acid Res. Mol. Biol.* **20**, 131–160
33. Worthylyake, D. K., Wang, H., Yoo, S., Sundquist, W. I., and Hill, C. P. (1999) *Acta Crystallogr. Sect. D Biol. Crystallogr.* **55**, 85–92